

1 Global long-term trends in the total electron content

2
3 Jaroslav Urbář, and Jan Laštovička

4 Institute of Atmospheric Physics, Czech Acad. Sci., Bocni II 1401, 14100 Prague, Czech Republic

5
6 *Correspondence:* Jan Laštovička (jla@ufa.cas.cz)

7
8 **Abstract.** The total electron content (TEC) is an important parameter for the ionospheric dynamics, GNSS/GPS
9 signal propagation and related applications of GNSS/GPS signals. Despite this fact the long-term trends in TEC
10 have been studied a little only. Here we analyze the homogeneous series JPL-35 of global TEC data for 1994-
11 2014 for selection of the optimum solar activity proxy for TEC analyses, and the UPC TEC data over 2003-2023
12 for estimating long-term trends in TEC. TEC trends are very predominantly negative. TEC trends reveal a clear
13 wavenumber 2 longitudinal structure in low/equatorial latitudes with strong negative trends in belts 0-60°E and
14 180-240°E and weak trends in 90-150°E and 270-330°E. For more detailed information on TEC trends a longer
15 series of reliable TEC data is required.

16 17 18 1 Introduction

19
20 The increasing atmospheric concentration of greenhouse gases, particularly of carbon dioxide, and long-term
21 changes of other trend drivers, mainly the secular change of the Earth magnetic field and of the stratospheric
22 ozone concentration, result in long-term trends in the thermosphere and ionosphere (e.g., Lastovicka et al.,
23 2012). Since the pioneering work by Rishbeth and Roble (1992) the investigations of long-term trends in the
24 ionosphere have been developing for more than 30 years. The state of investigations of long-term trends in the
25 mesosphere-thermosphere-ionosphere system has recently been reviewed by Lastovicka (2023).

26
27 One of the most important ionospheric parameters is the total vertical columnar electron content (TEC),
28 particularly due to its impact on propagation of signals of the Global Navigation Satellite Systems (GNSS) such
29 as the Global Positioning System (GPS) and their applications, e.g. precise positioning, causing serious issues for
30 the single-frequency receiver-based positioning and for precise positioning using differential GNSS techniques,
31 like (Network) Real Time Kinematic (RTK/NRTK) (Hernández-Pajares et al., 2017). Global TEC data are
32 available only since 1994; therefore trends in TEC have been studied less than trends in other main ionospheric
33 parameters observed by the global ionosonde network since the International Geophysical Year in 1957/58. The
34 first paper on trends in TEC was published by Lean et al. (2011) for the period 1995-2010. They found the
35 average trend to be positive, which is not consistent with trends in foF2. Lastovicka (2013) used historical (1976-
36 1996) Faraday rotation-based TEC data from Florence, Italy, the region where Lean et al. (2011) trends were
37 positive and much stronger than average trends. He found no long-term trend but with relatively large
38 uncertainty, which however questioned results of Lean et al. (2011). Lean et al. (2016) analyzed TEC data over
39 the period 1999-2015 and obtained a very weak, statistically insignificant global TEC trend (negative but close

40 to zero). Emmert et al. (2017) constructed homogeneous TEC data series JPL-35 based on 35 globally
41 distributed stations re-evaluated consistently by the same method. They compared the evolution of JPL-35 data
42 with other data series for 1994-2014. Emmert et al. (2017, their Fig. 7) found non-stable level of TEC in early
43 years, particularly jump up of CODE data series by 3 TECU in autumn 2001. Lastovicka et al. (2017) used
44 Emmert's JPL-35 global TEC data series and found slight negative trend in global TEC and provided evidence
45 that the Lean (2011) positive trend was a consequence of data problem in early years (before autumn 2001) of
46 TEC data series, and "better" result of Lean et al. (2016) is due to the fact that they included less "wrong" years
47 into analysis.

48

49 Before studying TEC trends we have to solve the problem of optimum solar activity proxy for removal the solar
50 cycle effect, because for foF2 it was found that trends are critically dependent on selection of the optimum solar
51 activity proxy (Lastovicka, 2024). This is the first task of this paper. F30 was found to be the optimum solar
52 activity proxy for foF2 (Lastovicka and Buresova, 2023; Danilov and Berbeneva, 2023, 2024; Zossi et al., 2023).
53 The main task of this paper is to establish the regional TEC long-term trends globally.

54

55 In this work we shall examine the regional TEC trends globally in dependence on latitude and longitude over the
56 globe. Section 2 describes data and methods used. Section 3 deals with the selection of optimum solar activity
57 proxy for TEC investigations. Section 4 treats long-term trends in TEC. Section 5 contains conclusions.

58

59

60 **2 Data and methods**

61

62 To reach the first goal, to select the optimum solar activity proxy, the Emmert's et al. (2017) homogeneous
63 global average TEC data JPL-35 will be used (Emmert et al., 2017, Supplement, Data Set S1). We shall analyze
64 yearly average values based on monthly medians over the period 1994-2014. Criteria used for selection of the
65 optimum solar activity proxy are described in section 3.

66

67 To study the regional long-term trends in TEC, the UPC TEC global map data are used (Hernandez-Pajares et
68 al., 1998). We analyze yearly averages based on monthly medians around noon (10-14 local time) for 2003-
69 2023. The time interval has been selected to avoid data problems. Before 2002 the TEC data from all
70 international resources (IGS, CODE, JPL, UPC, ESA) are more or less unstable according to Emmert et al.
71 (2017), whereas since 2002 they are stable with respect to JPL-35. Moreover, UPC data were issued with epoch
72 having time step of two hours, before 2003 in odd hours and since 2003 in even hours. Data are separated by two
73 hours in local time (LT). Therefore to have all data in the same LT, we are performing analysis for averages in
74 meridional belts thick 30° of longitude (equal to 2 hours of LT) with latitudinal step/resolution 2.5° . The first belt
75 is centered at 0°E , next at 30°E etc.

76

77 The long-term trends are calculated in the traditional way. First the effect of solar activity is removed from TEC
78 data in order to remove the much stronger solar cycle effect. Then the trends are calculated from TEC residuals
79 in the following way:

80 First, the dependence of TEC on solar proxies (i.e. parameters A and B) is calculated by linear regression, Eq.
 81 (1):

$$82 \quad \text{TEC} = A + B * \text{solar proxy} \quad (1)$$

83 Second, using Eq. (1) with parameters A and B calculated in the first step, model values of TEC_{mod} are
 84 calculated for all individual years and all solar proxies. Third, using linear regression for TEC residuals $\text{TEC}_{\text{obs}} -$
 85 TEC_{mod} , Eq. (2):

$$86 \quad \text{TEC}_{\text{obs}} - \text{TEC}_{\text{mod}} = C + D * \text{time} \quad (2)$$

87 where TEC_{obs} is the observed value of TEC, the long-term trend represented by the trend coefficient D is
 88 calculated.

91 3 Selection of the optimum solar activity proxy for TEC

92
 93 For the selection of the optimum solar activity proxy we use Emmert's (2017) homogenized TEC data JPL-35,
 94 1994-2014, and six solar activity indices/proxies, F10.7, F30, Mg II, He II, sunspot number and the solar Lyman-
 95 α flux. The optimum solar activity proxy selection requires criteria according to which the selection may be
 96 made. We use four such criteria:

- 97 1. Percentage of total variance of TEC described by solar activity proxy should be the largest one.
- 98 2. The standard error of trend slope/coefficient D should be the smallest one.
- 99 3. Percentage of total variance of TEC residuals ($\text{TEC}_{\text{obs}} - \text{TEC}_{\text{mod}}$) described by trend with the given solar proxy
 100 should be the largest one.
- 101 4. The average of absolute values of differences between observed and model (with solar proxy) TEC (TEC
 102 residuals) should be the smallest one.

103
 104 **Table 1.** Global TEC JPL-35, 1994-2014, the fulfillment of criteria of selection of the optimum solar activity
 105 proxy. R^2_{solar} - percentage of total variance of TEC described by solar activity proxy. Slope D and its standard
 106 error – trend coefficient. R^2_{trend} - Percentage of total variance of TEC residuals ($\text{TEC}_{\text{obs}} - \text{TEC}_{\text{mod}}$) described by
 107 long-term trend. dTEC - The average of absolute values of differences between observed and model (with solar
 108 proxy) TEC (TEC residuals).

	F10.7	F α	Mg II	sunspots	F30	He II
R^2_{solar}	99%	99%	99%	99%	99%	99%
Slope D (TECU/yr)	-0.048 ± 0.025	-0.060 ± 0.026	-0.067 ± 0.028	0.012 ± 0.032	-0.108 ± 0.024	0.100 ± 0.050
R^2_{trend}	0.16	0.21	0.23	0.01	0.52	0.21
dTEC	0.51	0.55	0.69	0.73	0.44	0.74

110
 111 Table 1 show how these criteria are fulfilled for all six solar activity proxies used. The first row presents the
 112 percentage of total variance of TEC described by individual solar activity proxies. These percentages are equal,
 113 99%, for all solar activity proxies, thus this criterion does not help to select the optimal proxy. However, 99%

114 confirms that the linear equation (1) may be used, that it is not oversimplification. The second row show the
 115 trend slope/coefficients and, more important, their standard errors. The smallest standard error (even though with
 116 the highest trend slope) is for F30 but those for F10.7, F α and Mg II differ very little. However, this criterion
 117 disqualifies He II. The third row brings information about the percentage of total variance of TEC residuals
 118 described by trend with individual solar activity proxies. This criterion clearly and very much favors F30
 119 (percentage for F30 is more than twice as large as for all other solar activity proxies) and evidently disqualifies
 120 sunspot numbers. The fourth criterion shown on the fourth row, the average of absolute values of differences
 121 between observed and model TEC, again supports F30 as the optimum solar activity proxy. Summing up, we
 122 may say that F30 is the optimum solar activity proxy for studying long-term trends of TEC based on yearly
 123 values. This result is not surprising, because F30 is also the optimum solar activity proxy for foF2 as discussed in
 124 Introduction and the F2 layer forms very substantial contribution to TEC.

125

126 **Table 2.** The same as Table 1 but for the global UPC TEC at noon, 2003-2023.

127

	F10.7	F α	Mg II	sunspots	F30
R ² solar	99%	95%	98%	97%	100%
Slope D (TECU/yr)	-0.019 ± 0.025	-0.069 ± 0.043	-0.085 ± 0.028	0.006 ± 0.035	-0.022 ± 0.013
R ² trend	3%	12%	33%	0%	12%
dTEC	0.52	0.86	0.69	0.77	0.32

128

129 In Table 2 we repeat search for the optimum solar activity proxy with the global UPC TEC calculated for noon
 130 (noon in all longitudinal bands, see section 4). The first row reveals the highest percentage of total variance to be
 131 described by the solar activity proxy F30 (100% means more than 99.5%) followed by F10.7 and Mg II and it
 132 disqualifies F α (only 95%). The smallest standard error in the second row is again for F30, even though the
 133 largest trend slope occurs with Mg II. A smaller trend slope for F30 might be the consequence of a very small
 134 part of non-solar total variance of TEC for F30 (less than 0.5%). This is probably also reason for smaller
 135 percentage of total variance of TEC residuals described by F30 than by Mg II on the third row; this row
 136 disqualifies sunspot numbers. The last row, which shows the average of absolute values of differences between
 137 observed and model TEC, again favors F30. So according to three out of four criteria again F30 is the optimum
 138 solar activity proxy.

139

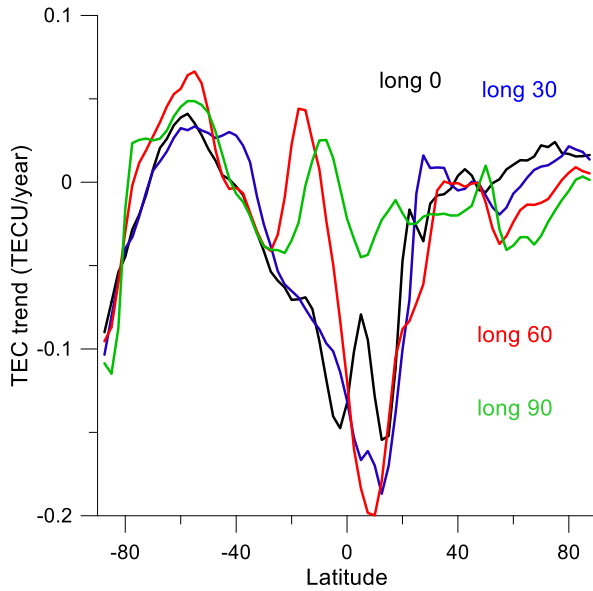
140

141 **4 Long-term trends in TEC**

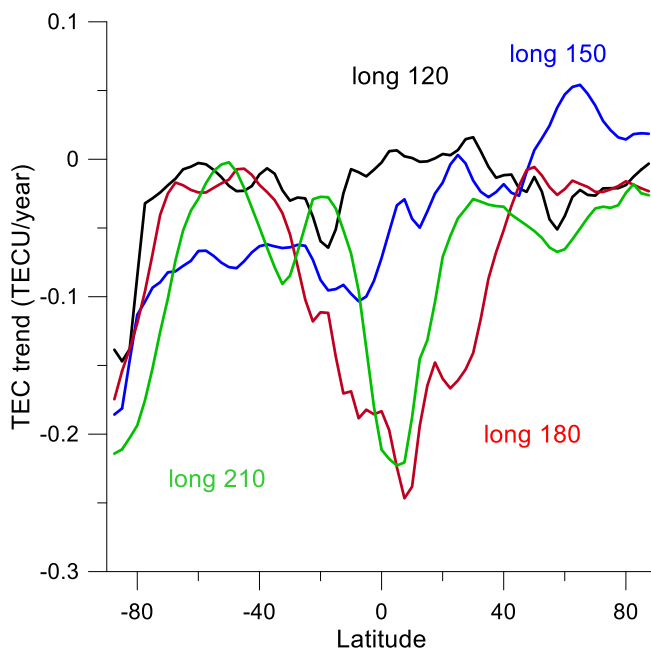
142

143 Since long-term trends in foF2 are most pronounced around noon (e.g., Danilov, 2015) and the F2 region
 144 represents very important contribution to TEC, we focus on TEC trends around noon (10-14 LT). They are
 145 calculated using equations (1) and (2) and solar activity proxy F30. These trends are presented in Figs. 1-3 in the
 146 form of meridional profiles of trends separated by 30° in longitude. All three Figures reveal a similar general
 147 latitudinal pattern. At higher latitudes ($\varphi > 30^\circ$, for Fig. 3 $\varphi > 20^\circ$) at both hemispheres the trends are weak, close

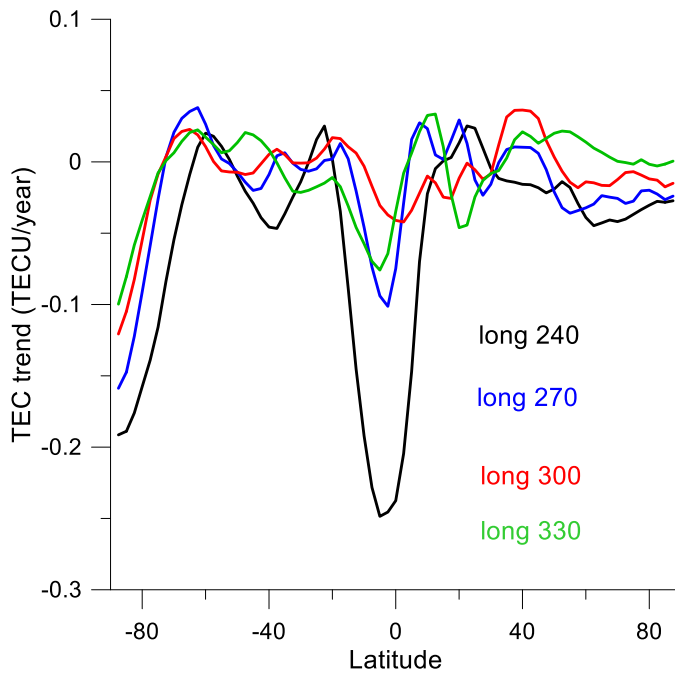
148 to no trend, and dominantly insignificant except for the southern very high latitudes, which display a larger
 149 negative trend; all longitudinal belts provide similar pattern. At lower latitudes the pattern is clearly different.
 150 Strong negative trends occur for longitudinal belts 0-60°E and 180-240°E. On the other hand, longitudinal belts
 151 90-150°E and 270-330°E reveal the same lower latitude pattern as higher latitude pattern, weak or no trends.
 152



153
 154 Fig. 1. Latitudinal dependence of TEC trends (TECU/year) for longitudinal belts centered at 0°, 30°, 60° and 90°,
 155 latitudes 87.5°S-87.5 N.
 156



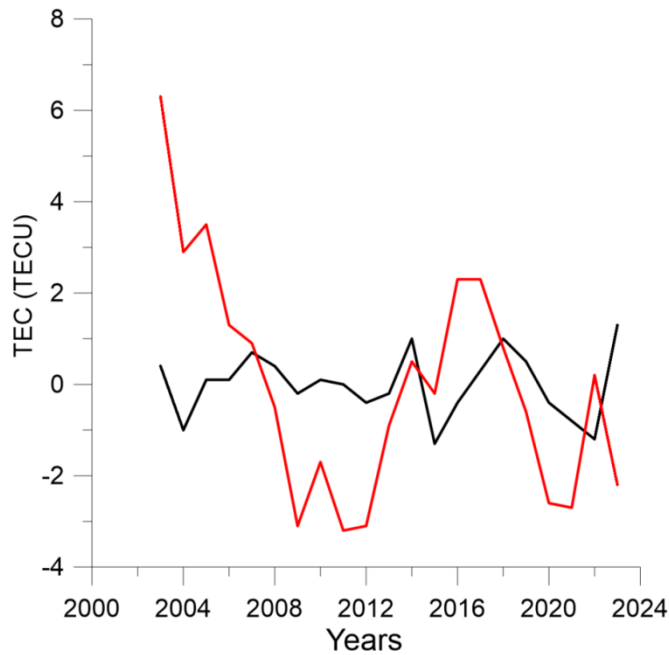
157
 158 Fig. 2. Latitudinal dependence of TEC trends (TECU/year) for longitudinal belts centered at 120°, 150°, 180° and
 159 210°, latitudes 87.5°S-87.5 N.
 160



161
 162
 163
 164
 165
 166
 167
 168
 169
 170
 171
 172
 173
 174
 175
 176
 177
 178
 179
 180
 181

Fig. 3. Latitudinal dependence of TEC trends (TECU/year) for longitudinal belts centered at 240°, 270°, 300° and 330°, latitudes 87.5°S-87.5°N.

Important compound of trend investigations is statistical significance of results. The statistical significance of TEC trends is predominantly low. Trends with significance higher than two standard deviations (2σ) occur for all profiles at southern very high latitudes (in average 80-87.5°S). Trend profiles with large low-latitude trends are significant at the 2σ level typically between 20°N and 20°S, whereas profiles with weak trends are significant only in the vicinity of equator and for some profiles only. Profiles with weak low-latitude trends are mostly statistically significant at the 2σ level also at northern higher middle latitudes (typically 50°-65°N). TEC trends appear to be statistically significant at southern very high latitudes ($\phi \geq 80^\circ\text{S}$), however these latitudes suffer with low density of data. All other parts of trend profiles reveal lower statistical significance, many of them even lower than 1σ . One reason for so low significance of linear trend might be change of trend during the analyzed period. To check this possibility, Fig. 4 shows temporal evolution of TEC residuals ΔTEC at 30°E for latitudes with the strongest (12.5°N) and weakest (40°N) trends. 40°N clearly reveals no change of trend and also 12.5°N does not show an evident change of linear trend. However, Fig. 4 displays large year-to-year variability of ΔTEC ; with such a large variability to get trends with sufficient statistical significance requires for most of trend values longer data sets. In this sense our results might be considered preliminary except for clear dominance of negative trends and a clear division of trends at low latitudes into four groups of strong and weak trends.



182 Fig. 4. Evolution of TEC residuals at 30°E, 40°N (black, no trend) and 12.5°N (red, the largest trend).

183
184
185 Andima et al. (2019) analyzed TEC trends for equatorial station Malindi in Kenya; our negative trend value for
186 this region is within the range of their trend values. More positive/less negative trends of global TEC by Lean et
187 al. (2011, 2016) are explained by the use of TEC data prior to 2002 without any correction. This data problem
188 was unknown at the time of publication of Lean's et al. results; it was detected first by Emmert et al. (2017).

189
190 As concerns model simulations of trends in TEC, our global JPL-35 TEC trend -0.108 ± 0.024 TECU/year (Table
191 1) calculated with F30 is somewhat higher than the trend simulated by Cnossen (2020, Table 1), which reached
192 values between -0.060 ± 0.012 and -0.024 ± 0.008 TECU/year, but trend calculated with F10.7 (-0.048 ± 0.025),
193 which was used by Cnossen (2020), are within the range of Cnossen (2020) trend values. The global UPC TEC
194 trend (Table 2) is at the lower end of range of Cnossen (2020) trends. McInerney et al. (2024) used model
195 WACCM-X to calculate TEC trends. They obtained for March and June, 1920-2010, zonal means, negative
196 trends of various magnitude at all latitudes. Thus our trends in global TEC at least qualitatively agree with the
197 trends from model simulations.

198 Why are low-latitude TEC trends separated into two longitudinally-separated groups of strong and weak trends?
199 Secular change of Earth's magnetic field does not seem to be responsible for the observed longitudinal structure
200 of the low latitude TEC trends, because it has pronounced impact on the low latitude ionospheric F2-region
201 trends in the 270-330°E belt (Qian et al., 2021), where TEC trends are weak. If the TEC trends shown in global
202 geographic coordinates are re-binned into the geomagnetic grid, this outcome will not change significantly.
203 Another possibility could be the effect of non-migrating tides. There is well-known effect of the DE3 non-
204 migrating tide on the low-latitude/equatorial ionosphere but it produces longitudinal structure with wavenumber
205 4, whereas TEC trends display longitudinal structure with the zonal wavenumber 2 at low/equatorial latitudes.
206 This problem requires more detailed study, which is out of the topic of this paper; it will be treated in future
207 investigations.

209
210
211
212
213
214
215
216
217
218
219
220
221
222
223
224
225
226
227
228
229
230
231
232
233
234
235
236
237
238
239
240
241
242
243
244
245
246
247
248

5 Conclusions

TEC is an important parameter for propagation and applications of GNSS/GPS signals. Despite this fact the long-term trends in TEC have been studied a little only. Altogether five papers dealt with trends in observed TEC until now (Lean et al., 2011, 2016; Lastovicka, 2013; Lastovicka et al., 2017; Andima et al., 2019) and their results are not mutually consistent. The results of this work may be summarized as follows:

1. The TEC trends are mostly statistically insignificant at the 2σ level, even though in some latitudinal-longitudinal regions they are statistically significant. This means that only gross features, not fine details, may be considered reliable. Longer data series is required for getting finer structure of TEC trends.
2. The optimum solar activity proxy for investigating long-term trends in TEC is F30, not F10.7, Mg II or sunspot numbers. This is consistent with F30 being the optimum solar proxy for foF2 trends (Lastovicka and Buresova, 2023).
3. The long-term TEC trends are very predominantly negative; all statistically significant trends are negative.
4. TEC trends reveal a clear zonal wavenumber 2 longitudinal structure in low/equatorial latitudes with strong negative trends in belts 0-60°E and 180-240°E and weak trends in 90-150°E and 270-330°E.

Future investigations will focus on analysis of longer data series and on search for explanation of longitudinal structure of TEC trends at low/equatorial latitudes.

Data availability.

Data used in this study are publicly available on the following websites:

Solar activity indices were taken from:

F10.7 (observed) - https://lasp.colorado.edu/lisird/data/noaa_radio_flux/,

F30 - <https://solar.nro.nao.ac.jp/norp/data/daily/>,

Lyman- α - https://lasp.colorado.edu/data/timed_see/composite_lya/version3/,

Mg II - <http://www.iup.uni-bremen.de/UVSAT/Datasets/mgii>,

sunspot numbers were taken from <https://sidc.be/silso/datafiles>,

He II - from the SOLID project database: [https://projects.pmodwrc.ch/solid-](https://projects.pmodwrc.ch/solid-visualization/makeover/index.php?type=proxy&waveStart=215&waveEnd=215&dateStart=1970-01-01&dateEnd=2014-12-31)

[visualization/makeover/index.php?type=proxy&waveStart=215&waveEnd=215&dateStart=1970-01-](https://projects.pmodwrc.ch/solid-visualization/makeover/index.php?type=proxy&waveStart=215&waveEnd=215&dateStart=1970-01-01&dateEnd=2014-12-31)

[01&dateEnd=2014-12-31](https://projects.pmodwrc.ch/solid-visualization/makeover/index.php?type=proxy&waveStart=215&waveEnd=215&dateStart=1970-01-01&dateEnd=2014-12-31), with the option: Proxies > Data selections > He II > Download.

Global TEC data were taken from Emmert et al. (2017), supporting information, Data Set S1].

UPC TEC data were taken from <https://cddis.nasa.gov/archive/gnss/products/ionex/2023/>.

Author contributions.

J.L.: Conceptualization, analysis of global TEC data. J.U.: Data mining and analysis of UPC TEC data. Both:

Writing of manuscript.

249 *Competing interests.* The contact author has declared that none of the authors has any competing interests.

250

251 *Acknowledgements:* We acknowledge work of all who contributed to production of ionospheric and solar data
252 used in this article. Support by the Czech Academy of Sciences via program Strategy 21, project Analysis of
253 relationship between solar activity induced and anthropogenic changes of climate of the upper atmosphere, is
254 acknowledged..

255

256

257 **References**

258

259 Andima, G., Amabayo, E. B., Jurua, E., Cilliers, P. J.: Modeling of GPS total electron content over the African
260 low-latitude region using empirical orthogonal functions. *Ann. Geophys.*, 37, 65-76, doi:10.5194/angeo-37-
261 65-2019, 2019.

262 Cnossen, I.: Analysis and attribution of climate change in the upper atmosphere from 1950 to 2015 simulated by
263 WACCM-X. *J. Geophys. Res. Space Phys.*, 125(12), e2020JA028623,
264 <https://doi.org/10.1029/2020JA028623>, 2020.

265 Danilov, A.D.: Seasonal and diurnal variations in foF2 trends, *J. Geophys. Res. Space Phys.*, 120, 3868–3882,
266 doi:10.1002/2014JA020971, 2015.

267 Danilov, A.D., and Berbeneva, N. A.: Statistical analysis of the critical frequency foF2 dependence on various
268 solar activity indices, *Adv. Space Res.*, 72, 2351-2361, <https://doi.org/10.1016/j.asr.2023.05.012>, 2023.

269 Danilov, A.D., and Berbeneva, N. A.: Dependence of foF2 on solar activity indices based on the data of
270 ionospheric stations of the Northern and Southern Hemispheres, *Geom. Aeron.*, 64, 224-234,
271 <https://doi.org/10.1134/S00167932203601035>, 2024.

272 Emmert, J. T., Mannucci, A. J., McDonald, S. E., and Vergados, P.: Attribution of interminimum changes in
273 global and hemispheric total electron content, *J. Geophys. Res. Space Phys.*, 122, 2424–2439,
274 <https://doi.org/10.1002/2016JA023680>, 2017.

275 Hernandez-Pajares, Juan, J. M., Sanz, J., and Sole, J.G.: Global observation of the ionospheric electronic
276 response to solar events using ground and LEO GPS data, *J. Geophys. Res. Space Phys.*, 103, A9, 20789–
277 20796, <https://doi.org/10.1029/98JA01272>, 1998.

278 Hernández-Pajares, M., Wielgosz, P., Paziewski, J., Krypiak-Gregorczyk, A., Krukowska, M., Stepniak, K.,
279 Kaplon, J., Hadas T., Sosnica K., Bosy J., Orus-Perez, R., Monte-Moreno E., Yang, H., Garcia-Rigo A., and
280 Olivares-Pulido, G.: Direct MSTID mitigation in precise GPS processing. *Radio Sci.*, 52, 321–337,
281 <https://doi.org/10.1002/2016RS006159>, 2017.

282 Lastovicka, J.: Are trends in total electron content (TEC) really positive? *J. Geophys. Res. Space Phys.*, 118,
283 3831–3835, doi:10.1002/jgra.50261, 2013.

284 Lastovicka, J.: Progress in investigating long-term trends in the mesosphere, thermosphere and ionosphere,
285 *Atmos. Chem. Phys.*, 23, 5783-5800, <https://doi.org/10.5194/acp-23-5783-2023>, 2023.

286 Lastovicka, J.: Dependence of long-term trends in foF2 at middle latitudes on different solar activity proxies,
287 *Adv. Space Res.*, 73, 685-689, <https://doi.org/10.1016/j.asr.2023.09.047>, 2024.

288 Lastovicka, J, and Buresova, D.: Relationships between foF2 and various solar activity proxies, *Space Weather*,
289 21(4), e2022SW003359, <https://doi.org/10.1029/2022SW003359>, 2023.

290 Lastovicka, J., Solomon, S. C., and L. Qian, L.: Trends in the neutral and ionized upper atmosphere, *Space Sci.*
291 *Revs.*, 168, 113–145, doi:10.1007/s11214-011-9799-3, 2012.

292 Lastovicka, J., Urbar, J., and Kozubek, M.: Long-term trends in the total electron content (TEC), *Geophys. Res.*
293 *Lett.*, 44, 8168–8172, doi:10.1002/2017GL075063, 2017.

294 Lean J., Emmert, J. T., Picone, J. M., and Meier, R. R.: Global and regional trends in ionospheric electron
295 content, *J. Geophys. Res.*, 116, A00H04, doi:10.1029/2010JA016378, 2011.

296 Lean, J. L., R. R. Meier, R. R., Picone, J. M., Sassi, F., Emmert, J. T., and Richards, P. G.: Ionospheric total
297 electron content: Spatial patterns of variability, *J. Geophys. Res. Space Phys.*, 121, 10367–10402, doi:
298 10.1002/2016JA023210, 2016.

299 McInerney, J. M., Qian, L., Liu, H.-L., Solomon, S. C., and Nossal, S. M.: Climate change in the thermosphere
300 and ionosphere from the early twentieth century to early twenty first century simulated by the Whole
301 Atmosphere Community Climate Model-eXtended. *J. Geophys. Res. Space Phys.*, 129, e2023JD039397, doi:
302 10.1029/2023JD039397, 2024.

303 Qian, L., McInerney, J. M., Solomon, S. S., Liu, H., and Burns, A. G.: Climate Changes in the Upper
304 Atmosphere: Contributions by the Changing Greenhouse Gas Concentrations and Earth's Magnetic Field
305 From the 1960s to 2010s. *J. Geophys. Res. Space Phys.*, 126, e2020JA029067,
306 <https://doi.org/10.1029/2020JA029067>, 2021.

307 Rishbeth, H., and Roble, R. G.: Cooling of the upper atmosphere by enhanced greenhouse gases – modeling of
308 thermospheric and ionospheric effects. *Planet. Space Sci.*, 40, 1011–1026, 1992.

309 Zossi, Z. S., Medina, F. D., Tan Jun, G., Lastovicka, J., Duran, T., Fagre, M., de Haro Barbas, B. F., and Elias,
310 A. G.: Extending the analysis on the best solar activity proxy for long-term ionospheric investigations, *Proc.*
311 *Roy. Soc. A – Math. Phys. Eng. Sci.*, 479:20230225, <https://doi.org/10.1098/rspa.2023.0225>, 2023.